Master Stability Functions for Synchronized Coupled Systems

Louis M. Pecora and Thomas L. Carroll
Code 6343, Naval Research Laboratory, Washington, D.C. 20375
(Received 7 July 1997)

We show that many coupled oscillator array configurations considered in the literature can be put into a simple form so that determining the stability of the synchronous state can be done by a master stability function, which can be tailored to one's choice of stability requirement. This solves, once and for all, the problem of synchronous stability for any linear coupling of that oscillator. [S0031-9007(98)05387-3]

PACS numbers: 05.45.+b, 84.30.Ng

A particularly interesting form of dynamical behavior occurs in networks of coupled systems or oscillators when all of the subsystems behave in the same fashion; that is, they all do the same thing at the same time. Such behavior of a network simulates a continuous system that has a uniform movement, models neurons that synchronize, and coupled synchronized lasers and electronic circuit systems. A central dynamical question is: When is such synchronous behavior stable, especially in regard to coupling strengths in the network? Interest in this question has been high over the last several years in both chaotic [1–11] as well as limit cycle systems [12–14]. Such studies typically assumed a particular form of coupling in the network and then analyzed the features of, stability of, and bifurcations from the synchronized state.

We have made progress toward developing a general approach to the synchronization of identical dynamical systems, building on the ideas of scaling in our previous work [15]. The consequence of this is a master stability equation, which allows us to calculate the stability (as determined from a particular choice of stability measure, like Lyapunov or Floquet exponents) *once and for all* for a particular choice of system (e.g., Rössler, Lorenz, etc.) and a particular choice of component coupling (e.g., x, y, etc.). Then, we can generate the stability diagrams for any other linear coupling scheme involving that system and component.

Any one system can have a wide variety of desynchronizing bifurcations. Using the master stability diagram, we can predict a diversity of spatial-mode instabilities including bursting or bubbling patterns [8]. The master stability diagram makes it obvious why particular coupling schemes may have an upper limit on the number of oscillators that can be coupled while still retaining a stable, synchronous state.

We assume the following: (1) The coupled oscillators (nodes) are all identical, (2) the same function of the components from each oscillator is used to couple to other oscillators, (3) the synchronization manifold is an invariant manifold, and (4) the nodes are coupled in an arbitrary fashion which is well approximated near the synchronous state by a linear operator. Numbers (1) and (3) guarantee the existence of a synchronization hyperplane in the phase space and number (2) makes the stability diagram specific to our choice of oscillators and the components. Number (4) is the choice of many studies of coupled systems since it is often a good approximation and can be considered prototypical.

In determining the stability of the synchronous state, various criteria are possible. The weakest is that the maximum Lyapunov exponent or Floquet exponent be negative. This is a universal stability standard, but it does not guarantee that there are not unstable invariant sets in the synchronous state [8] or areas on the attractor that are locally unstable [1,16,17], both of which can cause attractor bubbling and bursting of the system away from synchronization when there is noise or parameter mismatch. The theory we develop below will apply to almost any criterion that depends on the variational equation of the system. Each stability criterion will lead to its own master stability function. For that reason, we develop the theory in the context of Lyapunov exponents as a stability criterion and show in the conclusions how the other criteria can be used.

Let there be N nodes (oscillators). Let $\mathbf{x}^i$ be the m-dimensional vector of dynamical variables of the ith node. Let the isolated (uncoupled) dynamics be $\dot{\mathbf{x}}^i = \mathbf{F}(\mathbf{x}^i)$ for each node. $\mathbf{H}$: $R^m \rightarrow R^m$ is an arbitrary function of each node's variables that is used in the coupling. Thus, the dynamics of the ith node are $\dot{\mathbf{x}}^i = \mathbf{F}(\mathbf{x}^i) + \sigma \sum_j G_{ij}\mathbf{H}(\mathbf{x}^j)$, where σ is a coupling strength. The sum $\sum_j G_{ij} = 0$, so that assumption (3) above holds. The $N - 1$ constraints $\mathbf{x}^1 = \mathbf{x}^2 = \cdots = \mathbf{x}^N$ define the *synchronization manifold.*

Let $\mathbf{x} = (\mathbf{x}^1, \mathbf{x}^2, \ldots, \mathbf{x}^N)$, $\mathbf{F}(\mathbf{x}) = [\mathbf{F}(\mathbf{x}^1), \mathbf{F}(\mathbf{x}^2), \ldots, \mathbf{F}(\mathbf{x}^N)]$, $\mathbf{H}(\mathbf{x}) = [\mathbf{H}(\mathbf{x}^1), \mathbf{H}(\mathbf{x}^2), \ldots, \mathbf{H}(\mathbf{x}^N)]$, and $\mathbf{G}$ be the matrix of coupling coefficients $\{G_{ij}\}$, then

$$\dot{\mathbf{x}} = \mathbf{F}(\mathbf{x}) + \sigma \mathbf{G} \otimes \mathbf{H}(\mathbf{x}), \tag{1}$$

where $\otimes$ is the direct product. Note, we could start with a more general, nonlinear form in the coupling term and then assume that evaluation of the Jacobian of (1) leads to a constant matrix on the synchronization manifold. Either way, the analysis from here on follows the same pattern and we present (1) for its greater clarity.

Many coupling schemes are covered by Eq. (1). For example, if we use Lorenz systems for our nodes, $m = 3$.

If the coupling is through the Lorenz "x" component, then the function $\mathbf{H}$ is just the matrix

$$\mathbf{E} = \begin{pmatrix} 1 & 0 & 0 \\ 0 & 0 & 0 \\ 0 & 0 & 0 \end{pmatrix}.$$

Our choice of $\mathbf{G}$ will provide the connectivity of nodes. Equation (2) shows $\mathbf{G}$ for nearest-neighbor diffusive coupling and star coupling [18]. Similarly, all-to-all coupling has all 1's for G_{ij} $(i \neq j)$ and $-N + 1$ for G_{ii}. The boundary conditions are all cyclic in Eqs. (2), but many others are possible. The majority of coupling schemes treated in the dynamics literature can be put into the form of Eq. (1) by choosing the right $\mathbf{G}$ matrix.

$$\mathbf{G}_1 = \begin{pmatrix} -2 & 1 & 0 & \cdots & 1 \\ 1 & -2 & 1 & \cdots & 0 \\ 0 & 1 & -2 & \cdots & 0 \\ \vdots & \vdots & \vdots & \vdots & \vdots \\ 1 & 0 & \cdots & 1 & -2 \end{pmatrix},$$

$$\mathbf{G}_2 = \begin{pmatrix} -N+1 & 1 & 1 & \cdots & 1 \\ 1 & -1 & 0 & \cdots & 0 \\ 1 & 0 & -1 & \cdots & 0 \\ \vdots & \vdots & \vdots & \vdots & \vdots \\ 1 & 0 & \cdots & 0 & -1 \end{pmatrix}. \tag{2}$$

We get the variational equation of Eq. (1) by letting ξ^i be the variations on the ith node and the collection of variations is $\xi = (\xi^1, \xi^2, \ldots, \xi^N)$. Then,

$$\dot{\xi} = [\mathbf{1}_N \otimes D\mathbf{F} + \sigma \mathbf{G} \otimes D\mathbf{H}]\xi\,. \tag{3}$$

When $\mathbf{H}$ is just a matrix $\mathbf{E}$, $D\mathbf{H} = \mathbf{E}$. Equation (3) is used to calculate Floquet or Lyapunov exponents. We really want to consider only variations ξ which are transverse to the synchronization manifold. We want those variations to damp out. We next show how to separate out those variations and simplify the problem.

The first term in Eq. (3) is block diagonal with $m \times m$ blocks. The second term can be treated by diagonalizing $\mathbf{G}$. The transformation which does this does not affect the first term since it acts only on the matrix $\mathbf{1}_N$. This leaves us with a block diagonalized variational equation with each block having the form

$$\dot{\xi}_k = [D\mathbf{F} + \sigma\gamma_k D\mathbf{H}]\xi_k\,, \tag{4}$$

where γ_k is an eigenvalue of $\mathbf{G}$, $k = 0, 1, 2, \ldots, N-1$. For $k = 0$, we have the variational equation for the synchronization manifold ($\gamma_0 = 0$), so we have succeeded in separating that from the other, transverse directions. All other k's correspond to transverse eigenvectors. We can think of these as transverse modes and we will refer to them as such.

The Jacobian functions $D\mathbf{F}$ and $D\mathbf{H}$ are the same for each block, since they are evaluated on the synchronized state. Thus, for each k, the form of each block [Eq. (4)] is the same with only the scalar multiplier $\sigma\gamma_k$ differing for each. This leads us to the following formulation of the *master stability equation* and the associated *master stability function:* We calculate the maximum Floquet or Lyapunov exponents $\lambda_{\max}$ for the generic variational equation

$$\dot{\zeta} = [D\mathbf{F} + (\alpha + i\beta)D\mathbf{H}]\zeta \tag{5}$$

as a function of α and β. This yields the stability function $\lambda_{\max}$ as a surface over the complex plane [see Fig. 1, inset (a)]. Complex numbers are used since $\mathbf{G}$ may have complex eigenvalues. Then, given a coupling strength σ, we locate the point $\sigma\gamma_k$ in the complex plane. The sign of $\lambda_{\max}$ at that point will reveal the stability of that eigenmode—hence, we have a master stability function. If all of the eigenmodes are stable, then the synchronous state is stable at that coupling strength.

To illustrate, we chose chaotic Rössler systems [19] $(a = b = 0.2, c = 7.0)$ as the nodes and coupled them through the x component; thus, $\mathbf{H} = \mathbf{E}$ and $\mathbf{E}$ is as above. Figure 1 shows a contour plot of the master stability function for this oscillator. We see that there is a region of stability defined by a roughly semicircular shape. The plot is symmetric in the imaginary directions about the real axis. At $\alpha = \beta = 0$, $\lambda_{\max} > 0$ since this is just the case of isolated, chaotic Rössler systems. As α increases (with $\beta = 0$), $\lambda_{\max}$ crosses a threshold and becomes negative. Further increase in α reveals another threshold as $\lambda_{\max}$

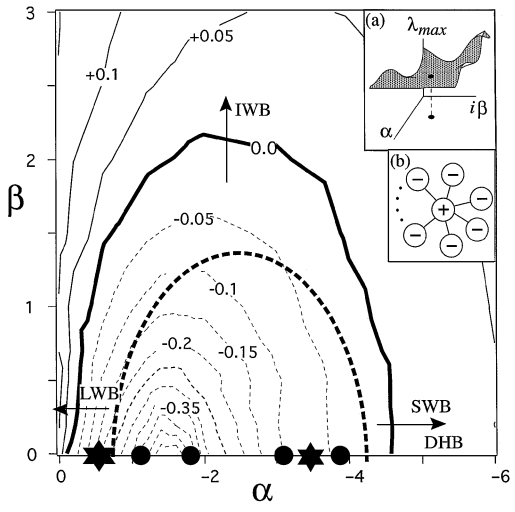

FIG. 1. Master stability function for x-coupled Rössler oscillators. Lightly dashed lines show contours of negative exponents and solid lines show contours of positive exponents. Circles show the eigenvalues for the diffusive coupling example. Stars show the eigenvalues for a star-coupled example. The bold, dotted semiellipse is the line of eigenvalues of an asymmetrically coupled Rössler system for particular coupling strengths. LWB, IWB, and SWB label long-wavelength, intermediate-wavelength, and short-wavelength bifurcations, respectively, that occur with diffusive-coupling schemes when eigenvalues cross the stability threshold. For the star configuration DHB labels a drum-head-mode bifurcation. Inset (a) shows a typical surface for the master stability function. Inset (b) shows the relation between the hub and spokes oscillators when a DHB takes place.

crosses over to become positive again. This implies that if the coupling is too strong the synchronous state will not be stable. If α is set to be in the stable range and β is increased, then $\lambda_{\max}$ can also cross a threshold and become positive, implying that a large imaginary coupling can destabilize the system. Imaginary eigenvalues arise from antisymmetric couplings (see below).

Diffusive coupling in a circular array [using the first $\mathbf{G}$ matrix in Eq. (2)] gives eigenvalues of $\gamma_k = 4\sin^2(\pi k/N)$, each twice degenerate and the eigenmodes are discrete sine and cosine functions of the node indices i [6,20]. For a particular coupling strength σ, we show the points $\sigma\ \gamma_k$ in Fig. 1 for an array of 10 Rösslers. The array has a stable synchronous state. As the coupling σ increases from 0, the first mode to become stable is the shortest spatial-frequency mode; the last mode to become stable is the longest spatial-frequency mode. Thus, in a stable, synchronous state, decreasing σ will cause a desynchronization with the long-wavelength mode going unstable first, a long-wavelength bifurcation (LWB). Increasing σ causes the shortest wavelength to become unstable, a short-wavelength bifurcation (SWB) [9,15].

Note, as more oscillators are added to the array, more transverse modes are created and the distance (along the real axis α) between the longest and shortest wavelength modes increases. Eventually, the system will reach a point at which we will increase σ to stabilize the long-wavelength mode only to have the short-wavelength mode become unstable at the same time. There will be an *upper limit* on the size of a stable, synchronous array of chaotic Rössler oscillators [9,15]. Such a size limit will *always* exist in arrays of chaotic oscillators with such limited stable regimes. Such a size limit will not exist if the oscillators are limit cycles, but the stable range of σ will be compressed down toward the origin as more oscillators are added to the array.

In all-to-all coupling schemes the transverse eigenvalues are all the same, $\gamma_k = -\sigma N$. The all-to-all scheme can support synchronous chaos for the Rössler oscillator example for the right σ. Unlike diffusive coupling, *all* modes become unstable when the threshold is crossed.

Star coupling [the second matrix in Eq. (2)—see inset (b) of Fig. 1] results in two eigenvalues, $\gamma_k = -\sigma$ and $\gamma_k = -\sigma N$. This yields two points on the master stability surface (see Fig. 1 for seven oscillators). If we decrease σ, we get a desynchronizing bifurcation in which sinusoidal modes that are on the spokes of the star become unstable and grow. If we increase σ, we get an interesting desynchronization bifurcation where the nodes on the spokes remain synchronous, but the hub node begins to develop motions of opposite sign to the former. We call this a drum-head bifurcation (see the inset in Fig. 1). There is also a size limit for the star configuration. For the x-coupled Rössler example, the maximum number of synchronized oscillators is 45.

We now consider a more complex coupling scheme with asymmetric nearest-neighbor coupling. We also add all-to-all coupling. The x coupling term in the Rössler example becomes $(c_s - c_u)x^{i+1} + (c_s + c_u)x^{i-1} - 2c_s x^i + c_a \sum_j (x^j - x^i)$. This is the sum of $\mathbf{G}_1$ [in Eq. (2)], $\mathbf{G}_2$ [Eq. (2)], and $\mathbf{G}_3$, an antisymmetric matrix with -1 on the row above the diagonal, $+1$ on the row below the diagonal, and zeros elsewhere. With each matrix is associated a coupling strength c_s, c_a, and c_u, respectively. The matrices are simultaneously diagonalizable using sinusoidal modes. The eigenvalues are complex (due to the antisymmetric part), $\gamma_k = -2c_s[1 - \cos(2\pi k/N)] + 2c_u i \sin(2\pi k/N) - c_a N$, and they must lie on an ellipse centered at $-2c_s - c_a N$ (see Fig. 1). We can always adjust the coupling strengths so all transverse eigenvalues lie in the stable region. Increasing c_s will elongate the ellipse along the real axis. Depending on where the ellipse is centered, this can cause either a LWB or a SWB. Increasing c_u can cause an intermediate wavelength bifurcation (IWB) for the Rössler situation, since the ellipse can elongate in the imaginary direction causing the intermediate wavelengths to become unstable (IWB).

We experimentally tested the dependence of bifurcation type (LWB, IWB, or SWB) as a function of couplings c_s and c_u using a set of eight coupled Rössler-like circuits [6] which have individual attractors with the same topology as the Rössler system in the chaotic regime. We initially set $c_s = 0.2$, $c_u = 0$, and $c_a = 0.1$ so that the Rössler circuits were in the synchronous state. We controlled the coupling constants c_s and c_u using a digital-to-analog convertor in a computer. The circuits were started in the synchronous state and then the coupling was instantaneously reset to new values of c_s and c_u. At the same time, we recorded the x signals from all eight oscillators simultaneously with a 12-bit eight-channel digitizer card. We arbitrarily chose the threshold of the sum of modes 1–4 exceeding 5% of the synchronous mode to determine when the oscillators were not in sync. More experimental information will be given elsewhere.

After we switched the coupling constants c_s and c_u from the synchronous state to a nonsynchronous state, we fit the transient portion of each mode-amplitude time series to an exponential function to find a growth rate λ for each mode. We recorded the mode with the largest λ as being the most unstable mode. Figure 2(a) shows the experimental results. In Fig. 2(b), we plot the least stable eigenmode found from the master stability function. Theory and experiment compare well. The synchronous region has a similar shape, including the sharp peak just before the SWB region. Other bifurcation regions agree reasonably well, including the small mode 3 region near the peak of the sync region.

We noted that other stability criteria are possible. Each will produce its own master function over the complex coupling plane. Among them are the following three: (1) Calculate the maximum Lyapunov exponent or Floquet multiplier for the least stable invariant set [8,17], e.g., an unstable periodic orbit in a chaotic attractor, (2) calculate the maximum (supremum) of the real part of the

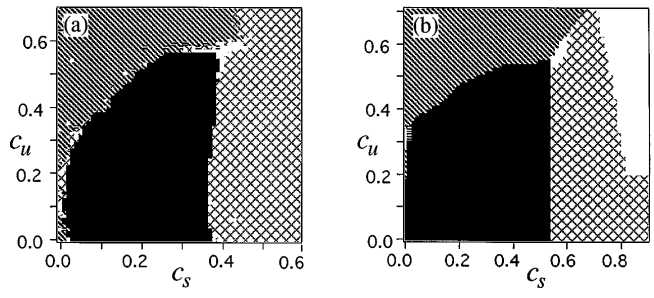

FIG. 2. (a) Plot of experimental results for asymmetrically coupled Rössler-like circuits showing the classes of desynchronizing bifurcations that occur when the symmetric (c_s) or antisymmetric (c_u) part of the coupling is changed from a synchronous state to a state in which the theory predicts that one of the eigenmodes should be unstable. The labeling scheme is ■ = synchronous mode, = = long wavelength (mode 1) \\ = intermediate wavelength (mode 2), white space = intermediate wavelength (mode 3), and × = short wavelength (mode 4). (b) Similar plot of theoretical prediction of which modes are least stable.

eigenvalues of the (instantaneous) Jacobian (including the coupling terms) at all points or some representative set of points on the attractor [16]; e.g., when negative, this function guarantees ultimate transverse-direction contraction everywhere on the attractor, and (3) calculate the maximum eigenvalue of the (instantaneous) symmetrized Jacobian (including the coupling terms) at all points or some representative set of points on the attractor [1]; e.g., this guarantees monotone damping of transverse perturbations [21]. Using the same analysis as above, criteria (1) and (2) come down to Eq. (5), although the evaluation of the stability function will be on the special, unstable invariant set or of the real part of the eigenvalue of the right-hand-side linear operator. Criterion (3) can also be analyzed in the same way provided there are some common restrictions. These, again, lead to a block diagonalization of the variational equation in the same way as before with the final stability function being the maximum eigenvalue on the attractor of the linear operator $\dot{\zeta} = [D\mathbf{F} + D\mathbf{F}^T + (\alpha + i\beta)D\mathbf{H}]\zeta$ [22]. Many other stability criteria, such as the recently introduced Brown-Rulkov criterion [23,24] will also produce a master stability function. Which one to use depends on one's requirements.

The master stability function allows one to quickly establish whether *any* linear coupling arrangement will produce stable synchronous dynamics. In addition, it reveals which desynchronization bifurcation mode will occur when the coupling scheme or strength changes. Attractor bubbling or bursting behavior [8] shows up mainly as bursts of the particular mode or modes that are closest to instability. Using Eq. (5) for large α or β, we can explain why the synchronous state is unstable for certain systems in the asymptotic limit of large real or imaginary coupling. Finally, the coupling need only be locally linear for there to be a master stability function; i.e., the form of the variational equation is similar to Eq. (3) near the synchronization manifold. The latter is a more common scenario. The issues in this last paragraph will be covered in more detail elsewhere.

[1] D. J. Gauthier and J. C. Bienfang, Phys. Rev. Lett. **77**, 1751 (1996).
[2] H. Fujisaka and T. Yamada, Prog. Theor. Phys. **69**, 32 (1983).
[3] V. S. Afraimovich, N. N. Verichev, and M. I. Rabinovich, Izv. Vyssh. Uchebn. Zaved. Radiofiz. **29**, 1050–1060 (1986).
[4] A. R. Volkovskii and N. F. Rul'kov, Sov. Tech. Phys. Lett. **15**, 249–251 (1989).
[5] J. M. Kowalski, G. L. Albert, and G. W. Gross, Phys. Rev. A **42**, 6260 (1990).
[6] J. F. Heagy, T. L. Carroll, and L. M. Pecora, Phys. Rev. E **50**, 1874 (1994).
[7] H. G. Winful and L. Rahman, Phys. Rev. Lett. **65**, 1575 (1990).
[8] P. Ashwin, J. Buescu, and I. Stewart, Phys. Lett. A **193**, 126–139 (1994).
[9] J. F. Heagy, T. L. Carroll, and L. M. Pecora, Phys. Rev. Lett. **73**, 3528 (1994).
[10] J. F. Heagy, T. L. Carroll, and L. M. Pecora, Phys. Rev. E **52**, R1253 (1995).
[11] A. S. Pikovskii, Radiophys. Quantum Electron. **27**, 390–394 (1984).
[12] N. Kopell and G. B. Ermentrout, Math. Biosci. **90**, 87 (1988).
[13] Y. Kuramoto, in *International Symposium on Mathematical Problems in Theoretical Physics*, Lecture Notes in Physics Vol. 39, edited by H. Araki (Springer-Verlag, Berlin, 1975), pp. 420–422.
[14] S. Watanabe and S. H. Strogatz, Phys. Rev. Lett. **70**, 2391 (1993).
[15] J. F. Heagy, L. M. Pecora, and T. L. Carroll, Phys. Rev. Lett. **74**, 4185 (1995).
[16] L. Pecora, T. Carroll, and J. Heagy, *Chaotic Circuits for Communications, Photonics East, SPIE Proceedings, Philadelphia, 1995* (SPIE, Bellingham, WA, 1995), Vol. 2612, pp. 25–36.
[17] N. F. Rulkov and M. M. Sushchik, Int. J. Bifurcation Chaos **7**, 625 (1997).
[18] For star coupling, one oscillator sits at the hub of a circular network and the other oscillators are coupled to the hub, but not to each other. See Fig. 1, inset (b).
[19] O. E. Rössler, Phys. Lett. **57A**, 397 (1976).
[20] D. Armbruster and G. Dangelmayr, Math. Proc. Camb. Philos. Soc. **101**, 167 (1987).
[21] Tomasz Kapitaniak, Int. J. Bifurcation Chaos **6**, 211 (1996).
[22] Following Ref. [1], we require $d\|\xi\|/dt < 0$ everywhere. Using $\|\xi\| = \xi^2$, we get the criterion $\xi^T(A^T + A)\xi < 0$, where A is the right-hand-side linear operator of Eq. (3). Employing the symmetry requirement on $D\mathbf{H}$ easily leads to block diagonalization and the final form shown. An alternate requirement for block diagonalization is that $\mathbf{G}$ and $\mathbf{G}^T$ commute.
[23] R. Brown and N. F. Rulkov, Phys. Rev. Lett. **78**, 4189 (1997).
[24] R. Brown and N. F. Rulkov, Chaos **7**, 395 (1997).